

Plasmonic core-shell metal-organic nanoparticles enhanced dye-sensitized solar cells

Qi Xu, Fang Liu,* Weisi Meng, and Yidong Huang

State Key Lab. of Integrated Optoelectronics, Department of Electronic Engineering, Tsinghua University, Beijing 100084, China

*liu_fang@tsinghua.edu.cn

Abstract: We present an investigation on introducing core-shell Au@PVP nanoparticles (NPs) into dye-sensitized solar cells. As a novel core-shell NPs structure, Au@PVP present not only the chemical stability to iodide/triiodide electrolyte, but also the adhesiveness to dye molecules, which could help to localize most of dye molecules around plasmonic NPs, hence increasing the optical absorption consequently the power conversion efficiency (PCE) of the device. We obtain a PCE enhancement of 30% from 3.3% to 4.3% with incorporation of Au@PVP NPs. Moreover, the device performance with different concentration of Au@PVP NPs from 0 to 12.5 wt% has been studied, and we draw the conclusion that the performance of DSCs could be well improved through enhancing the light absorption by local surface plasmon (LSP) effect from Au@PVP NPs with an optimized concentration.

©2012 Optical Society of America

OCIS codes: (040.0040) Detectors; (040.5350) Photovoltaic.

References and links

1. B. O'Regan and M. Grätzel, "A Low-Cost, High-Efficiency Solar Cell Based on Dye-Sensitized Colloidal TiO₂ Films," *Nature* **353**(6346), 737–740 (1991).
2. M. K. Nazeeruddin, A. Kay, I. Rodicio, R. Humphry-Baker, E. Mueller, P. Liska, N. Vlachopoulos, and M. Grätzel, "Conversion of Light to Electricity by cis-X₂bis (2,20-bipyridyl-4,40-dicarboxylate) ruthenium(II) Charge-Transfer Sensitizers(X = Cl-, Br-, I-, CN-, and SCN-) on Nanocrystalline Titanium Dioxide Electrodes," *J. Am. Chem. Soc.* **115**(14), 6382–6390 (1993).
3. M. Grätzel, "Photoelectrochemical cells," *Nature* **414**(6861), 338–344 (2001).
4. M. Grätzel, "Dye-sensitized solar cells," *J. Photochem. Photobiol. Photochem. Rev.* **4**(2), 145–153 (2003).
5. C. Y. Chen, M. Wang, J. Y. Li, N. Pootrakulchote, L. Alibabaei, C. H. Ngoc-le, J. D. Decoppet, J. H. Tsai, C. Grätzel, C. G. Wu, S. M. Zakeeruddin, and M. Grätzel, "Highly Efficient Light-Harvesting Ruthenium Sensitizer for Thin-Film Dye-Sensitized Solar Cells," *ACS Nano* **3**(10), 3103–3109 (2009).
6. R. Alvarez-Puebla, L. M. Liz-Marzan, and F. J. Garcia de Abajo, "Light Concentration at the Nanometer Scale," *J. Phys. Chem. Lett.* **1**(16), 2428–2434 (2010).
7. H. Nabika, M. Takase, F. Nagasawa, and K. Murakoshi, "Toward Plasmon-Induced Photoexcitation of Molecules," *J. Phys. Chem. Lett.* **1**(16), 2470–2487 (2010).
8. A. L. Koh, A. I. Fernández-Domínguez, D. W. McComb, S. A. Maier, and J. K. W. Yang, "High-Resolution Mapping of Electron-Beam-Excited Plasmon Modes in Lithographically Defined Gold Nanostructures," *Nano Lett.* **11**(3), 1323–1330 (2011).
9. L. Slaughter, W. S. Chang, and S. Link, "Characterizing Plasmons in Nanoparticles and Their Assemblies with Single Particle Spectroscopy," *J. Phys. Chem. Lett.* **2**(16), 2015–2023 (2011).
10. M. G. Blaber, A. I. Henry, J. M. Bingham, G. C. Schatz, and R. P. Van Duyne, "LSPR Imaging of Silver Triangular Nanoprisms: Correlating Scattering with Structure Using Electrodynamics for Plasmon Lifetime Analysis," *J. Phys. Chem. C* **116**(1), 393–403 (2012).
11. E. Thimsen, F. Le Formal, M. Grätzel, and S. C. Warren, "Influence of plasmonic Au nanoparticles on the photoactivity of Fe₂O₃ electrodes for water splitting," *Nano Lett.* **11**(1), 35–43 (2011).
12. C. Noguez, "Surface Plasmons on Metal Nanoparticles: The Influence of Shape and Physical Environment," *J. Phys. Chem. C* **111**(10), 3806–3819 (2007).
13. M. Ihara, K. Tanaka, K. Sakaki, I. Honma, and K. Yamada, "Enhancement of the Absorption Coefficient of cis-(NCS)₂ Bis(2,20-bipyridyl-4,40-dicarboxylate) ruthenium(II) Dye in Dye-Sensitized Solar Cells by a Silver Island Film," *J. Phys. Chem. B* **101**(26), 5153–5157 (1997).
14. K. Ishikawa, C. J. Wen, K. Yamada, and T. Okubo, "The Photocurrent of Dye-Sensitized Solar Cells Enhanced by the Surface Plasmon Resonance," *J. Chem. Eng. of Jpn* **37**(5), 645–649 (2004).
15. C. Hagglund, M. Zach, and B. Kasemo, "Enhanced Charge Carrier Generation in Dye Sensitized Solar Cells by Nanoparticle Plasmons," *Appl. Phys. Lett.* **92**(1), 013113 (2008).

16. S. D. Standridge, G. C. Schatz, and J. T. Hupp, "Toward Plasmonic Solar Cells: Protection of Silver Nanoparticles Via Atomic Layer Deposition of TiO₂," *Langmuir* **25**(5), 2596–2600 (2009).
17. S. D. Standridge, G. C. Schatz, and J. T. Hupp, "Distance Dependence of Plasmon-Enhanced Photocurrent in Dye-Sensitized Solar Cells," *J. Am. Chem. Soc.* **131**(24), 8407–8409 (2009).
18. G. Zhao, H. Kozuka, and T. Yoko, "Effects of the Incorporation of Silver and Gold Nanoparticles on the Photoanodic Properties of Rose Bengal Sensitized TiO₂ Film Electrodes Prepared by Sol-Gel Method," *Sol. Energy Mater. Sol. Cells* **46**(3), 219–231 (1997).
19. C. Wen, K. Ishikawa, M. Kishima, and K. Yamada, "Effects of Silver Particles on the Photovoltaic Properties of Dye-Sensitized TiO₂ Thin Films," *Sol. Energy Mater. Sol. Cells* **61**(4), 339–351 (2000).
20. M. D. Brown, T. Suteewong, R. S. S. Kumar, V. D'Innocenzo, A. Petrozza, M. M. Lee, U. Wiesner, and H. J. Snaith, "Plasmonic Dye-Sensitized Solar Cells Using Core-Shell Metal-Insulator Nanoparticles," *Nano Lett.* **11**(2), 438–445 (2011).
21. J. Qi, X. Dang, P. T. Hammond, and A. M. Belcher, "Highly Efficient Plasmon-Enhanced Dye-Sensitized Solar Cells Through Metal@Oxide Core@Shell Nanostructure," *ACS Nano* **5**(9), 7108–7116 (2011).
22. C. Nahm, H. Choi, J. Kim, D. R. Jung, C. Kim, J. Moon, B. Lee, and B. Park, "The effects of 100 nm-diameter Au nanoparticles on dye-sensitized solar cells," *Appl. Phys. Lett.* **99**(25), 253107 (2011).
23. P. V. Kamat, M. A. Fox, and A. J. Fatiadi, "Dye-loaded polymer electrodes. 2. Photoelectrochemical sensitization by croconate violet in polymer films," *J. Am. Chem. Soc.* **106**(5), 1191–1197 (1984).
24. P. V. Kamat and M. A. Fox, "Photophysics and photochemistry of xanthene dyes in polymer solutions and films," *J. Phys. Chem.* **88**(11), 2297–2302 (1984).
25. H. Chen, M. G. Blaber, S. D. Standridge, E. J. DeMarco, J. T. Hupp, M. A. Ratner, and G. C. Schatz, "Computational Modeling of Plasmon-Enhanced Light Absorption in a Multicomponent Dye Sensitized Solar Cell," *J. Phys. Chem. C* **116**(18), 10215–10221 (2012).
26. A. J. Moulé, H. J. Snaith, M. Kaiser, H. Klesper, D. M. Huang, M. Grätzel, and K. Meerholz, "Optical description of solid-state dye-sensitized solar cells. I. Measurement of layer optical properties," *J. Appl. Phys.* **106**(7), 073111 (2009).
27. D. M. Huang, H. J. Snaith, M. Grätzel, K. Meerholz, and A. J. Moulé, "Optical description of solid-state dye-sensitized solar cells. II. Device optical modeling with implications for improving efficiency," *J. Appl. Phys.* **106**(7), 073112 (2009).
28. A. C. Khazraji, S. Hotchandani, S. Das, and P. V. Kamat, "controlling Dye (Merocyanine-540) Aggregation on Nanostructured TiO₂ Films. An Organized Assembly Approach for Enhancing the Efficiency of Photosensitization," *J. Phys. Chem. B* **103**(22), 4693–4700 (1999).
29. S. Y. Huang, G. Schlichthörl, A. J. Nozik, M. Grätzel, and A. J. Frank, "Charge Recombination in Dye-Sensitized Nanocrystalline TiO₂ Solar Cells," *J. Phys. Chem. B* **101**(14), 2576–2582 (1997).
30. B. V. Enustun and J. Turkevich, "Coagulation of Colloidal Gold," *J. Am. Chem. Soc.* **85**(21), 3317–3328 (1963).
31. J. B. Khurgin, G. Sun, and R. A. Soref, "Practical limits of absorption enhancement near metal nanoparticles," *Appl. Phys. Lett.* **94**(7), 071103 (2009).
32. G. Sun, J. B. Khurgin, and R. A. Soref, "Practical enhancement of photoluminescence by metal nanoparticles," *Appl. Phys. Lett.* **94**(10), 101103 (2009).

1. Introduction

Dye-sensitized solar cells (DSCs) have attracted much great attention in recent years. The power conversion efficiency (PCE) of DSCs with mesoporous TiO₂ layer covered by a monolayer of dye molecules can reach a high value up to 11% and the cost of materials and fabrication processes is relatively low [1–5]. Plasmonic nanoparticles (NPs) have been employed as an attractive approach to boost the performance of DSCs due to their local surface plasmon (LSP) effect [6–12], which can enhance the light absorption and consequently increase the overall efficiency of the device [13–17]. Due to the recombination of photogenerated carriers and corrosion of electrolytes, the bare metal NPs, which direct contact with the dye and the electrolyte, cannot perform well on improving the total performance of the DSCs [18, 19]. Core-shell NPs have been applied to enhance PCE by preventing the recombination and corrosion. Earlier literatures have reported that Au@SiO₂ NPs were applied [20], then A. M. Belcher et. al. chose Ag@TiO₂ NPs instead of insulating components SiO₂ as the shell material, for the carriers generated by dye molecules located on the shell can be easily transferred to surrounding porous TiO₂ [21]. Because the concentration of plasmonic NPs doped into porous TiO₂ layers is limited to a relatively low level [22] and most of the dye molecules will not be located closely around the plasmonic NPs, only a small amount of dye molecules in TiO₂ layers could be influenced by the enhanced optical field. It is predictable that improving the utilization efficiency of LSP enhanced optical field can increase the overall efficiency of the solar cells further. Although there have been several papers published in this field up to now, most of which are on the thermal and structural

stability of the core-shell NPs [20], how to improve the utilization efficiency of LSP enhanced optical field is seldom involved.

In this paper, a novel core-shell metal-organic Au@PVP (PVP, poly (4-vinylpyridine)) NP is proposed and investigated. Au@PVP NPs have not only the abilities to avoid corrosion of metal NPs and recombination of carriers, which the common core-shell metal-inorganic NPs already have, but also the ability of adhesion to small molecules [23]. The utilization efficiency of LSP enhanced optical field can be improved due to the adhesion of Au@PVP NPs to more dye molecules around the NPs where the optical field is enhanced. Besides, Au@PVP NPs have other additional advantages, such as increase the lifetimes of the dye molecules [24]. Our research demonstrated that, by introducing Au@PVP NPs, the PCE of dye-sensitized solar cells is enhanced 30% from 3.3% to 4.3%. And the optimized concentration for getting best utilization efficiency of LSP enhanced optical field is also investigated.

2. Geometric design, synthesis, and characterization of core-shell Au@PVP nanoparticles

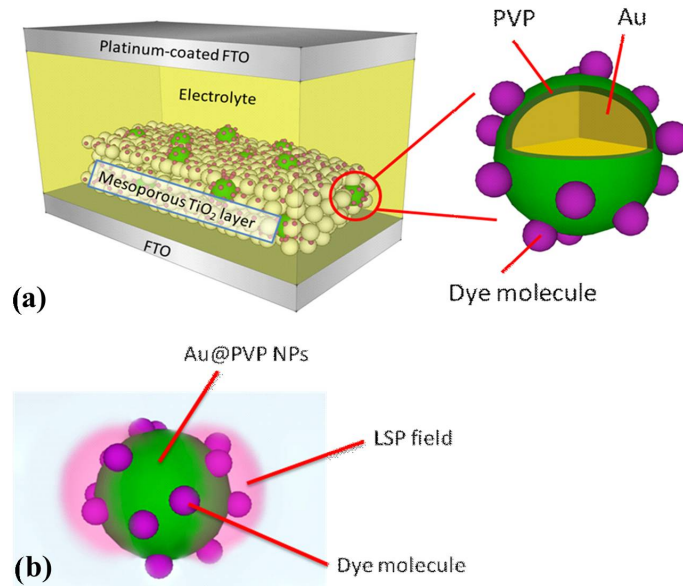


Fig. 1. Structures and mechanisms of plasmonic enhanced DSCs with core-shell Au@PVP NPs. (a) Structures of core-shell Au@PVP NPs and plasmonic enhanced DSCs. (b) Mechanisms of LSP from Au@PVP NPs enhancing dye absorption.

The structure of the Au@PVP NPs and plasmonic enhanced DSCs are shown in Fig. 1(a). Here, the Au@PVP NPs are embedded in the mesoporous TiO₂ layer and the LSPs arising from Au@PVP NPs increase the optical absorption of dye molecules. PVP has the advantages of not only readily forming films, which makes it good as a coating, but also can electronically and chemically protect the metals from the recombination and corrosion. Besides, PVP have the unique ability of adhesion to dye molecules (~2-3nm), which help to trap masses of dye molecules surrounding the metal NPs surface, hence the LSP field from metal sphere can affect sufficient dye molecules, as shown in Fig. 1(b), resulting in a significant enhancement on the optical absorption and overall efficiency of the DSCs. Moreover, Au@PVP NPs can also increase the lifetimes of the dye molecules, which will make considerable contribution to the enhancement of the device performance [24].

A theoretical investigation on spatial properties of light trapping by LSP effect is developed. Finite Element Method (FEM) is applied to calculate the LSP field distribution.

Figure 2(a) shows the intensity of electrical field $|E|^2$ of Au@PVP NPs in TiO₂ layer of DSCs with an incident planewave at $\lambda_0 = 600\text{nm}$ in a 3-dimensional model. The color map represents the intensity distribution of the electrical field and the color bar shows the intensity normalized by the maximum. The radius of Au core and the thickness of PVP shell are set to be 10nm and 1nm, respectively, and the material properties are obtained from earlier literatures [25–27]. The electromagnetic field is localized closely around the plasmonic NPs for the LSP effect. Figure 2(b) shows the optical absorption enhancement versus the distance from the surface of Au@PVP NPs along the radial direction. The optical absorption $A(r)$ is actually the average optical absorption in a very thin spherical shell with radius of r and thickness of $\Delta r = 1\text{nm}$ and normalized with the volume of the spherical shell $V(r)$, which can be calculated as:

$$A(r) = \frac{\frac{1}{2} \omega \epsilon_0 \int_V \text{Im}[\epsilon \cdot |E(r)|^2] dV}{V(r)} \quad (1)$$

where ϵ is the complex relative dielectric permittivity, E is the electric field, ω is the angular frequency, ϵ_0 is the permittivity in free space, r_0 is the radius of Au@PVP (here $r_0 = 11\text{nm}$), r is the radius of integrate sphere, hence $r - r_0$ is the distance from the surface along the radial direction. $V(r) = \frac{4\pi}{3} [(r + \Delta r)^3 - r^3]$ is the volume of integrate spherical shell.

And the optical absorption enhancement (OAE) can be obtained by:

$$OAE(r) = \frac{A_{\text{with Au@PVP}}(r)}{A_{\text{without Au@PVP}}(r)} \quad (2)$$

It can be seen that the optical intensity decreases dramatically when it get away from the surface of NPs, which indicate that only the dye molecules located closely enough to the plasmonic NPs can be sufficiently affected by LSP effect, while the others are hardly affected. Hence if there are sufficient dye molecules located closely to the plasmonic NPs that most of them are in intensive affection of LSP field, the optical absorption will be effectively increased and the device performance will be well improved. Utilizing PVP as the shell material will help to locate sufficient dye molecules closely to the plasmonic NPs surface due to its adhesion.

Besides the adhesion to small molecules, Au@PVP NPs can also increase the lifetimes of dye molecules [24]. The lifetimes of excited dyes can be extended by enclosing the dyes into a PVP polymer matrix, which will raise their abilities to participate in electron transfer or sensitization by energy transfer, hence to improve the photoelectronic properties of the device. Additionally, PVP can be employed as an electroactive polymer to transport charges, which would help to transfer the photogenerated carriers to the anode [28, 29].

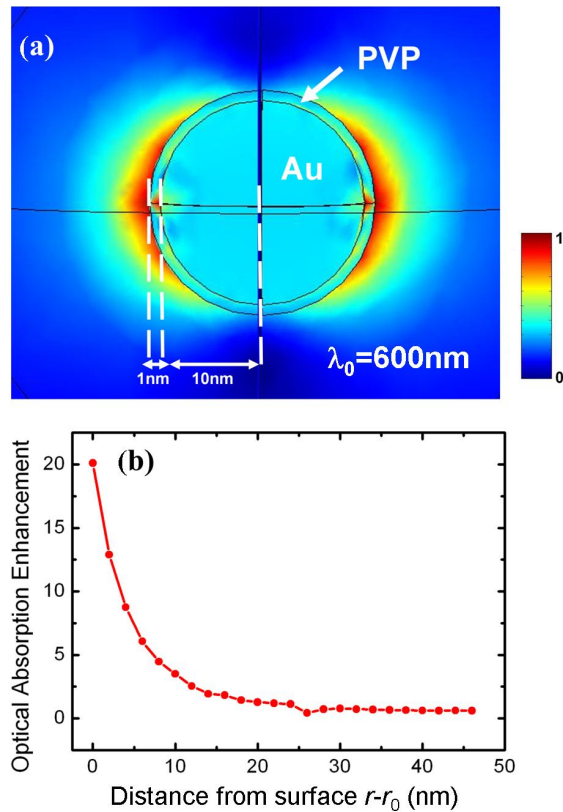


Fig. 2. Investigation on spatial properties of light trapping by LSP effect. (a) The intensity of electrical field $|E|^2$ of plasmonic Au@PVP NPs in TiO_2 layer with an incident planewave at $\lambda_0 = 600\text{nm}$. (b) Optical absorption enhancement versus the distance from surface of Au@PVP NPs

To fabricate Au@PVP core-shell NPs, monodisperse gold NPs are prepared according to the method described in Ref [30]. Briefly, an aqueous solution containing HAuCl_4 (purchased from Sigma-Ardrich) is heated to its boiling point under vigorous stirring, and then a sodium citrate solution is injected quickly into the system to cool down to room temperature. An aqueous solution of PVP (purchased from Sigma-Ardrich) is added to the colloidal gold solution to modify the gold NPs surface to facilitate PVP coating. The solution is stirred for 18-24h at room temperature. The PVP-coating gold NPs are collected by centrifugation and redispersed in deionized water or ethanol by sonication.

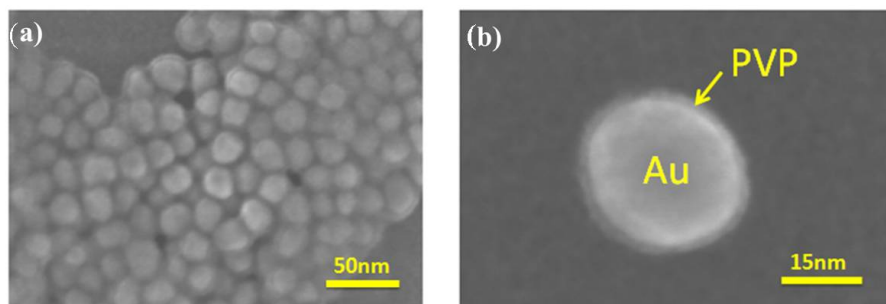


Fig. 3. Scanning electron microscopy (SEM) images of Au@PVP core-shell NPs before (a) and after (b) sonication.

Figure 3 shows the scanning electron microscopy (SEM, 30 kV, HITACHI S-5500) images of the Au@PVP core-shell NPs before a) and after b) sonication. It is observed that the diameter of gold sphere is about 20nm and the thickness of PVP shell is about 2-3nm, and the NPs assemble closely before sonication due to the adhesion of PVP.

To investigate the chemical stability of PVP polymer to the electrolyte containing iodide/triiodide redox couple, a preliminary experiment has been done to verify whether PVP can protect Au from the corrosion of electrolyte. Here, 50 μ L electrolyte (EL-HPE, Dyesol) containing iodide/triiodide redox couple is injected into 5mL bare Au colloidal solution and 5mL Au@PVP collosol solution followed by sonication, respectively. The molar ratio of Au element in these two solutions is the same. Figure 4(a) shows the appearance variation of colloidal Au and Au@PVP NPs versus time after mixed with electrolyte. Colloidal Au and Au@PVP NPs both appear wine-red under room light, due to the absorption maximum of colloidal Au and Au@PVP NPs at about 521 nm. After injected with electrolyte and simultaneously, the red colloidal Au NPs immediately turn to black in 2-3 minutes, and then gradually fade and become transparent, with presumption that corrosion occurs on Au NPs by iodide/triiodide redox couple. On the other aspect, Au@PVP NPs reveal a distinct resistance to corrosion of iodide/triiodide redox couple. After injected with electrolyte, the solution remains wine-red and last for more than one month. This experiment demonstrates that the PVP as a protective shell can notably restrain electrolyte to react with Au core.

To make a further confirm on this phenomenon, the optical absorption spectroscopy measurements are performed by using a UV-vis spectrophotometer (HITACHI U-3010). Figure 4(b) and 4(c) shows the optical absorption of bare Au NPs and Au@PVP NPs mixed with electrolyte containing iodide/triiodide redox couple. In Fig. 4(b), the characteristic absorption peak at about 521nm of Au NPs disappear after mixed with electrolyte, due to the corrosion of iodide/triiodide redox couple. Nevertheless, the optical absorption curve of Au@PVP NPs shown in Fig. 4(c) remains almost unchanging in intensity, which indicates the excellent chemical stability of PVP shell to electrolyte containing iodide/triiodide redox couple. And the tiny red shift of the red curve results from the refractive index change by injecting electrolyte.

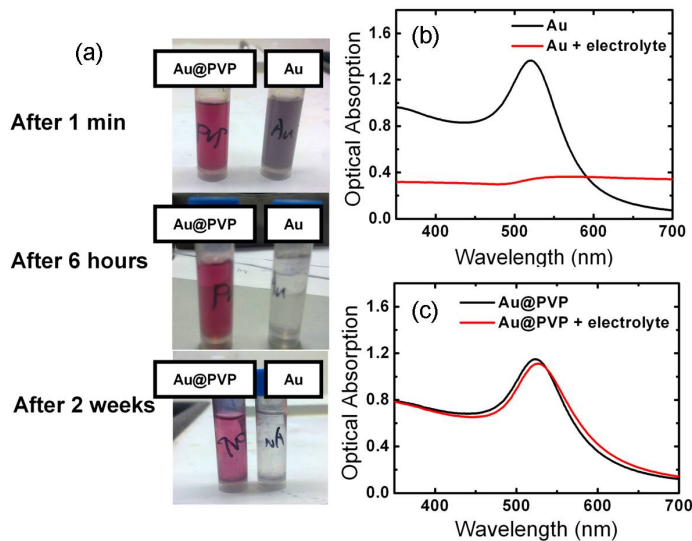


Fig. 4. Investigation of the chemical stability of Au/Au@PVP NPs. (a) Appearance variation tendency of Au and Au@PVP colloidal NPs versus time after mixed with electrolyte. (b) Optical absorption of bare Au NPs before/after mixed with electrolyte. (c) Optical absorption of Au@PVP NPs before/after mixed with electrolyte.

3. Optical absorption enhancement of dye molecule by Au@PVP NPs

To investigate the LSPs effect of Au@PVP NPs on the absorption of dye molecules, we studied light absorption enhancement of dye by blending Au@PVP or Au NPs in ethanol solution with precisely controlled concentrations of NPs and dyes, which can simulate the LSP effect in plasmon-enhanced DSCs.

Figure 5(a) shows the optical absorption spectra of Au NPs, Au@PVP NPs, N719 dye molecules, mixture of Au NPs and dye, mixture of Au@PVP and dye in ethanol solution. The light absorption of dye increases a lot with the presence of Au and Au@PVP NPs in solution with the same molar ratio. And the absorption of dye molecule mixed with Au@PVP NPs is much higher than that with bare Au NPs, which could be attributed to the adhesion of PVP polymer to dye molecules resulting in the large overlap of LSP enhanced electromagnetic field and dye molecules.

Figure 5(b) and 5(c) present the net changes (ΔOA) and relative changes ($\Delta\alpha/\alpha$) of dye absorption due to the presence of Au and Au@PVP NPs in solution, respectively. The two maximum peaks of absolute absorption enhancement of dye (N719) occurs at 375nm and 525 nm shown as the black curve in Fig. 5(a), and the net changes of dye absorption (ΔOA) present two maximum peaks at same positions when mixed with Au NPs or Au@PVP NPs. The optical absorption of dye molecules assisted by Au@PVP NPs is increased more significantly than that by bare Au NPs, suggesting that the PVP shell can trap more dye molecules around the NPs and overall optical absorption of dye can be significantly increased. To be noticed, surrounding these two absorption peaks of dye, the relative absorption enhancement $\Delta\alpha/\alpha$ present two troughs, which can be explained by the theory analysis that light absorption enhancement of active materials with LSP effect is more significantly when its original absorption ability is low [31, 32].

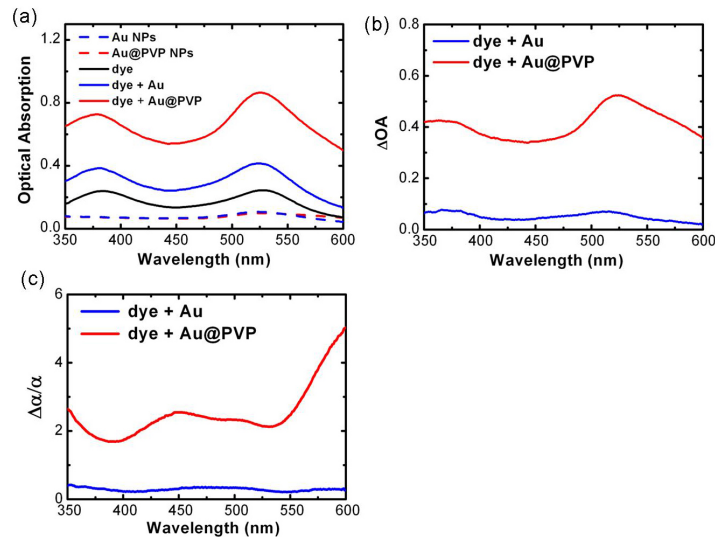


Fig. 5. LSP enhancement of optical absorption of Au/Au@PVP NPs and dye molecules in solution. (a) Optical absorption spectra of Au NPs, Au@PVP NPs, N719 dye molecules, mixture of Au NPs and dye, mixture of Au@PVP and dye in ethanol solution. (b) Net changes of dye absorption (ΔOA) due to the presence of Au/Au@PVP NPs in solution. (c) Relative changes of dye absorption ($\Delta\alpha/\alpha$) due to the presence of Au/Au@PVP NPs in solution. For the calculation of ΔOA and $\Delta\alpha/\alpha$: $\Delta\alpha/\alpha = \Delta OA(\lambda)/OA_{dye}(\lambda) = (OA_{dye,Au/Au@PVP}(\lambda) - OA_{dye}(\lambda) - OA_{Au/Au@PVP}(\lambda))/OA_{dye}(\lambda)$, Where $OA_{dye}(\lambda)$, $OA_{Au/Au@PVP}(\lambda)$, and $OA_{dye,Au/Au@PVP}(\lambda)$ are the optical absorption at wavelength λ of pure dye solution, Au/Au@PVP NPs solution, and their mixture solution with the same concentrations of dye and Au/Au@PVP NPs, respectively.

4. Fabrication and measurement of Au@PVP NPs enhanced DSCs

The TiO₂ paste purchased from Dyesol for fabricating photoanodes is dispersed in ethanol (TiO₂ paste to ethanol volume ratio about 1:1). To fabricate the TiO₂ photoanodes of DSCs, the TiO₂ paste is spin-coated on the FTO glass substrate with the conditions of 1800r/min for 40 seconds, dried at 125°C for 5min, and then annealed at 500°C for 15 min. While heating up (rate: 50°C/min), the photoanode turns brown and then becomes transparent. The thickness is about 3μm according to Dektak 150 surface profiler.

Considering the melting point of PVP polymer (about 170°C) is lower than the annealing temperature for photoanodes fabrication (up to 500°C), and with the intention of dispersing the Au@PVP NPs into the TiO₂ layer homogeneously, direct spin coating of Au@PVP NPs solutions onto TiO₂ layer is employed prior to sensitization of dye. The Au@PVP NPs in ethanol solution with different concentrations are prepared, and smeared onto the TiO₂ layer by spin coating at the condition of 600r/min for 20 seconds, followed by natural drying to remove the ethanol. The dye sensitization after the incorporation of Au@PVP NPs can help the dye molecules be adequately attached on both the TiO₂ and Au@PVP. Therefore, the PVP can help to “seize” additional dye molecules around Au@PVP NPs, compared with the DSCs without Au@PVP.

The following fabrication procedures are the same as that of the conventional DSCs. The photoanodes of TiO₂-only and those infiltrated with Au@PVP NPs are immersed into N719 dye (purchase from dyesol) solution and kept at room temperature for 24h. Then the impregnated photoanodes are put in ethanol for 5 min to remove non-adsorbed dye, followed by natural air drying. The device is sealed by sealing frame (Surlyn sealant) and injected with electrolyte (EL-HPE, Dyesol).

To investigate the effect of LSPs on DSCs performance, plasmon-enhanced DSCs with Au@PVP NPs and standard DSCs with only TiO₂ NPs as photoanodes are compared. The TiO₂-only DSCs are fabricated using the conventional method [20], while the Au@PVP NPs in different concentration are added into TiO₂ photoanode according to the method described above.

After the fabrication, the current-voltage characteristics of DSCs are measured under AM 1.5G illumination with solar simulator (91192, Oriel, USA). The power of the simulated light is calibrated to 1000 W/m², and the I-V curves are obtained by applying an external bias to the cell and measuring the generated photocurrent with a digital source meter. The incident photon-to-electron conversion efficiency (IPCE) spectra is obtained by using an IPCE measurement system (PECS20, Peccell Technologies, Inc., Japan) consisting of a 150 W xenon lamp light source and a monochromator in the resolution of 2nm. The incident photon flux is determined by using a calibrated silicon photodiode (Certificated Si-diode BQ-S1337).

Figure 6(a) and 6(b) shows the photocurrent density-voltage characteristics (J-V curves) and power conversion efficiency (PCE) of plasmon-enhanced DSCs with Au@PVP NPs and TiO₂-only DSCs with the same photoanode thickness of 3μm, respectively. Varying the concentration of Au@PVP NPs in DSCs, it is observed that the plasmon-enhanced DSCs exhibits a maximum PCE up to 4.3%, which is increased by about 30% compared with 3.3% of TiO₂-only DSCs. In Fig. 6(a), the open-circuit voltage (V_{oc}) of plasmon-enhanced DSCs and TiO₂-only DSCs are almost the same, while the short-circuit current density (J_{sc}) significantly increased by introducing Au@PVP NPs. According to the equation $\eta = J_{sc} \cdot V_{oc} \cdot FF / P_0$, where P₀ is the intensity of incident light, the improvement of PCE in the plasmon enhanced DSCs mainly caused by the increase of photocurrent thanks to the enhanced light absorption of dye with the help of LSPs.

From Fig. 6(b), we can see the dependence of PCE on the concentration of Au@PVP NPs in TiO₂ photoanode. The concentration of Au@PVP NPs in ethanol solution can be readily adjusted, and the Au@PVP:TiO₂ mass ratio approximately equals the mass of TiO₂ layer dividing that of Au@PVP NPs deposited onto the layer. When increasing the concentration of Au@PVP NPs, the PCE monotonically increases until the concentration reaches 7.5 wt%, and then decreases if further increasing Au@PVP NPs concentration. The PCE decreasing

may be caused by increased trapping of photogenerated electrons when high concentration Au@PVP NPs is introduced. Similar results can be found in Ref [22]. Hence, the performance of DSCs has been well improved through enhancing the light absorption and photocurrent by LSP effect from Au@PVP NPs with an optimized concentration.

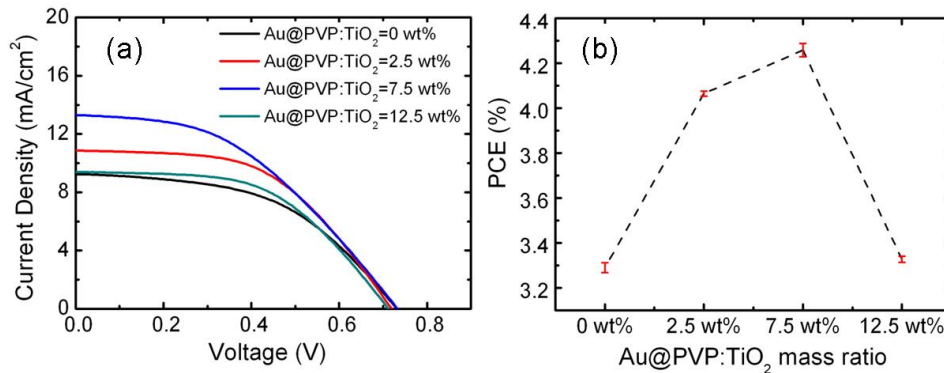


Fig. 6. Performance of TiO₂-only DSCs and core-shell NPs enhanced DSCs. (a) The photocurrent density-voltage characteristics (J-V curves) of TiO₂-only DSCs and core-shell NPs enhanced DSCs with different concentration of Au@PVP NPs with the same photoanode thickness of 3 μm. (b) Dependence of power conversion efficiency (PCE) on the concentration of Au@PVP NPs in TiO₂ photoanode with the same thickness of 3 μm. Here, four groups of Au@PVP NPs in different concentrations of 0 wt%, 2.5wt%, 7.5wt% and 12.5wt% are prepared and the PCE results are obtained from an average value of at least 6 samples for each concentration.

To investigate LSP effect on the spectral response of solar cells, the IPCE measurement is performed. Figure 7(a) shows the IPCE spectra of TiO₂-only DSCs and core-shell NPs enhanced DSCs with different concentration of Au@PVP NPs. It is indicated that the IPCE of core-shell NPs enhanced DSCs is increased over the whole wavelength range, especially within 400-600nm, compared with that of TiO₂-only DSCs. The IPCE is related with the light-harvesting efficiency, electron injection efficiency, and carrier collection efficiency simultaneously. Assuming the electron injection and collection are seldom affected, the increase of the IPCE should be attributed to the light harvest enhancement due to the LSP effect of core-shell NPs. The IPCE ratio of core-shell NPs enhanced DSCs to TiO₂-only DSCs shown in Fig. 7(b) illustrates that the enhancement is significant in the range of 400-600 nm. There is a peak at about 520nm in each line, which is consistent with the Au NP's resonance feature peak (about 523nm). The intensity of the peaks is different, which is related with the different photon-electric conversion performance of these samples. The optimized sample (Au@PVP:TiO₂ = 7.5 wt %) shows a highest peak at ~520 nm. Therefore, the measured IPCE also indicates that the LSPs of Au@PVP NPs improved the DSCs performance by increasing the optical absorption of dye molecules.

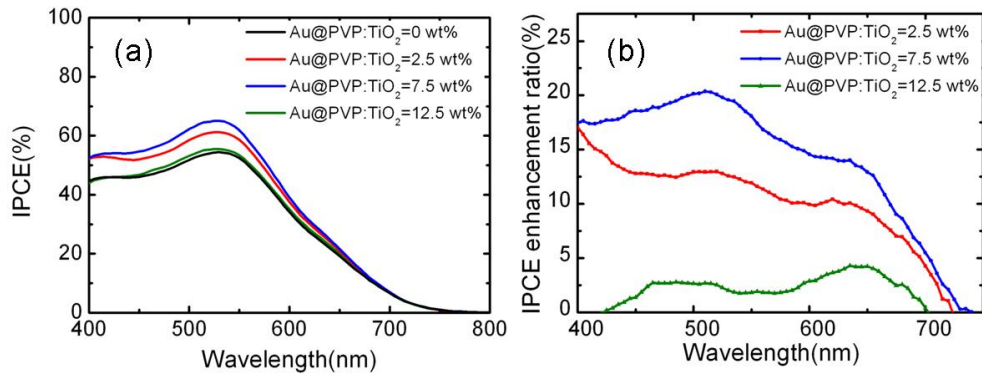


Fig. 7. Spectral responses of TiO₂-only DSCs and core-shell NPs enhanced DSCs with the same photoanode thickness of 3 μm. (a) IPCE spectra of TiO₂-only DSCs and core-shell NPs enhanced DSCs with different concentration of Au@PVP NPs. (b) the IPCE enhancement ratio of TiO₂-only DSCs and core-shell NPs enhanced DSCs with different concentration of Au@PVP NPs. IPCE enhancement ratio=(IPCE_{core-shell NPs}(λ)-IPCE_{TiO₂-only}(λ))/IPCE_{TiO₂-only}(λ) •100%, where IPCE_{core-shell NPs}(λ) and IPCE_{TiO₂-only}(λ) are the IPCE at wavelength λ for core-shell NPs enhanced DSCs and TiO₂-only DSCs, respectively.

5. Conclusions

In summary, we present the plasmon-enhanced DSCs by introducing core-shell Au@PVP NPs. The Au@PVP NPs comprised of metal core and PVP organic shell present not only the chemical stability to iodide/triiodide electrolyte, but also the adhesion to dye molecules to fully make use of the enhanced electromagnetic field of LSP and hence increase the PCE of DSCs. The experiment has been carried out by incorporating Au@PVP NPs with different concentration into the DSCs. And it is observed that the PCE of DSCs is improved by 30% from 3.3% to 4.3%. According to measured light absorption of dye and the IPCE of DSCs with Au@PVP NPs, we draw the conclusion that the performance of DSCs could be well improved through enhancing the light absorption hence the photocurrent by LSP effect of Au@PVP NPs with an optimized concentration.

Acknowledgments

This work was supported by the National Basic Research Programs of China (973 Program) under Contract No. 2011CB301803, No. 2010CB327405 and No. 2011CBA00608, the National High-tech R&D Program (863 Program) under Contract No. 2011AA050504, and the National Natural Science Foundation of China (NSFC-61036011, NSFC-61107050, and NSFC-61036010). The authors would like to thank Prof. Jiangde Peng, Prof. Wei Zhang, Dr. Xue Feng, and Kaiyu Cui, as well as Mr. Hiroki Tsujimura, and Yoshiaki Oku of ROHM Corporation for their helpful comments.